NIFS--144

JP9211116

Helical Divertor in the Large Helical Device

N. Ohyabu, N. Noda, Hantao JI, H. Akao, K. Akaishi, T. Ono,
H. Kaneko, T. Kawamura, Y. Kubota, S. Morimoto, A. Sagara,
T. Watanabe, K. Yamazaki and O. Motojima

(Received – Apr. 8, 1992)

NIFS-144 May 1992

Helical Divertor in the Large Helical Device

N. OHYABU, N. NODA, HANTAO JI, H. AKAO[1], K. AKAISHI, T. ONO[2], H. KANEKO, T. KAWAMURA, Y. KUBOTA, S. MORIMOTO, A. SAGARA, T. WATANABE, K. YAMAZAKI, O. MOTOJIMA

National Institute for Fusion Science, Nagoya, 464-01, Japan

[1] NEC Inc.

[2] Nagoya University

Abstract

The Large Helical device (LHD), now under construction is a Heliotron/torsatron device with a closed divertor system. The edge LHD magnetic structure has been studied in detail. A peculiar feature of the configuration is existence of edge surface layers, a complicated three dimensional magnetic structure. However it does not seem to hamper the expected divertor functions. As a confinement improvement scheme in LHD, we have proposed a high temperature divertor plasma operation in which a divertor plasma with temperature of a few kev, generated by efficient pumping, leads to the confinement improvement. Conceptual designs of the LHD divertor components are under way.

key words: helical divertor, high temperature divertor plasma , torsatron, LHD helical device, confinement enhancement

1. Introduction

With the inherent advantage of the stellarator as an attractive steady state reactor, there has been growing interest in the sterallator in the fusion community. The National Institute for Fusion Science (NIFS) is constructing a large, l = 2 Heliotron/torsatron device, called the Large Helical Device (LHD), aiming at demonstration of attractiveness of the helical device at more reactor relevant plasma parameters [1]. The LHD device parameters are : R (the major radius) = 3.9 m, a (the minor radius) = 0.6 m, m (the toroidal mode number of the helical coil) = 10, γ_c (the pitch of the helical coils) = 1.25. It is a superconducting coil device and thus steady state plasma operations will be demonstrated provided that the impurity contamination can be kept low. For this purpose, a kind of divertor is believed to be required for the impurity control. The divertor is also critically important in enhancing the core energy confinement [2].

The Heliotron/torsatron device has a built-in divertor configuration. This advantage has not been explored in any existing helical device partly because a full divertor configuration makes the device size larger and hence more expensive. The LHD device will be the first helical device which will demonstrate various divertor functions which enhance the plasma quality.

2. Features of the edge magnetic configuration

Divertor magnetic configuration in LHD is quite different from those in tokamaks. It is fairly complex and three dimensional and hence understanding of the magnetic structure is very important in designing the LHD divertor and predicting its performance. The LHD diverter

structure at the poloidal plane(constant ϕ plane) is shown in Fig.1(a). However it tends to be misleading since the divertor regions are helically twisted strongly. When one sees the divertor structure along the helical direction as in Fig.1(b), it looks like those of tokamaks even though the structure varies fairly strongly with toroidal angle ϕ due to strong toroidal effects.

Fig.2 shows an edge magnetic structure of a Heliotron/torsatron configuration. In the outer region just outside the closed surface region, several island layers with toroidal mode number of 10 are imbedded and with increasing radius, the poloidal mode number of the island layers decreases and the size of the island increases. Eventually the layers overlap, resulting in a stochastic field region. Thus definition of the outermost flux surface is vague. Beyond the stochastic region , there exists a region with multiple thin curved layers (the edge surface layer region). Fig.2 is a puncture plot of the field line tracing with starting points just within the stochastic region. Field lines from the stochastic region enter these surface layers and after many toroidal circulations, they reach "separatrix" with X-points and then hit the divertor plate. The existence of such edge surface layers is a peculiar feature of this type of divertor configuration.

To explain how this magnetic structure is created, we show movement of field lines on an edge surface layer labeled "1" in Fig.3(b). As they travel forwards by one toroidal pitch (36^{o} toroidally), they rotate poloidally just as those within the closed surface region do, moving on to the adjacent layer labeled "2". However, ones near the wall (i.e.,beyond the "separatrix") escape to the wall. When the field line moves into the region with $-(3/2)\pi < \theta < 0$ (where θ (the poloidal angle) is the angle

around the minor axis), the X-point moves radially inwards, approaching the layers. As a result, the field lines are pulled towards the X-point and bending of the surface layers (labeled "3") occurs. Field lines on the tip of the bended layer(e.g. field line C) are pulled towards the divertor plate. Variation in radial location of the X-point relative to the outermost flux surface with the poloidal angle is a key role in bending and folding the layers (Fig.3(a) shows clear difference in X-point radial location between $\theta = 0$ and $\theta = \pi$). Field line B and D rotates poloidally faster than field line A and E because of larger radius and hence higher local rotational transform. In this process, a sort of mixing takes place. Before the mixing, Field line A is located at the largest radius and the largest poloidal angle among the five field lines. After this process, it locates at smaller radius and smaller poloidal angle. Such folded layers are stretched into a very thin layer because the local rotational transform and the local shear are high near the "separatrix". Finally it becomes an "original" layer, but it is not at the same poloidal plane. With such a generation mechanism of the layer, any edge surface layer consists of multiple, extremely stretched layers, which themselves are a group of multiple layers.

Refering to Fig.2, there exist regions without the puncture points between the layers, meaning that the field lines in these regions are not connected to the stochastic region . Instead they are connected to the divertor plates when they are traced forwards and backwards. A group of the field lines in region 0 moves into region 1 after one toroidal pitch(36° toroidal rotation) and move into region 2 and so on, finally reaching the divertor plate. If field line is followed backwards, those in region 0 move back into region -1 after 36° backward toroidal rotation

and move into region -2 and so on, reaching the divertor plate.

Divertor operation with a high density, cold divertor plasma [3,4], is suitable to reduce the impurity sputtering and to enhance the edge radiation, a promising boundary control which we plan to pursue in the LHD experiments. One of the key divertor geometric parameters is the field line length between the scrape-off layer surrounding the main plasma region and the divertor plate. Longer connection length provides easier conditions for non-zero temperature gradient along the field line, which leads to lower temperature and higher density in front of the divertor plate. The length that field lines take to pass through the edge surface layer region is more than several times toroidal circumference, comparable to or even greater than a typical connection length in tokamaks. The vague boundary including the stochastic region and the edge surface layer region has a property of poor confinement and thus may serve to provide an edge radiative volume to reduce the heat flux on the divertor plate [4]. But the vague boundary may in turn prevent formation of the H-mode edge temperature pedestal, which leads to improvement of the core energy confinement. This has motivated us to propose a high temperature divertor plasma operation, discussed in the following section.

3. High temperature divertor plasma operation

A high temperature divertor plasma operation has been proposed to improve the energy confinement of the LHD plasma [5]. In this operational mode, the divertor plasma temperature is raised by efficient pumping in the divertor chamber. An elevated divertor temperature will lead to improvement of the core plasma.

In the high temperature divertor plasma operation mode, the edge

temperature is kept high by the pumping. The divertor temperature (T_{div}) is estimated by a power balance in the divertor channel. We consider a steady-state discharge which is heated (Q_{in}(input power)) and fuelled (Γ_{in}(particle flux)) by neutral beam injection alone, illustrated in Fig.4. We assumed that the pumping efficiency of the divertor is ξ , i.e., a fraction (ξ) of the particles reaching the divertor plates (Γ_{div}) are pumped and the same amount of the particles need to be fuelled by the neutral beam injection i.e., $\xi \cdot \Gamma_{div} = \Gamma_{in}$. The injected power(Q_{in}) into the main plasma region flows into the divertor channel and at the sheath of the divertor plate, a power balance ($Q_{in} = \gamma \cdot T_{div} \cdot \Gamma_{div}$) is satisfied where γ is the heat transmission coefficient. From these relations, the divertor temperature is given as $T_{div} = (Q_{in} / \Gamma_{in}) \cdot \xi / \gamma$. For a parameter set (beam energy(Q_{in} / Γ_{in}) ~ 100kev, $\gamma \sim 10$, $\xi \sim 0.2$), T_{div} becomes as high as 2 keV, significantly higher than those observed at the pedestal of H-mode discharges.

In this operation, a peaked density profile is maintained by a combination of deep fuelling such as pellet or neutral beam injection and particle pumping. Thus the diffusion coefficient (D) and hence the particle confinement becomes important in determining the energy confinement. This is desirable for the energy confinement in LHD where high neoclassical ripple induced electron heat loss(1/ν-regime) tends to suppress the temperature gradient. However the effective D is not high because the ions are confined by EXB drift (ν-regime). The radial electric field in such a plasma regime is positive and hence neoclassical outward impurity pinch [6] may prevent the impurity contamination. When this operation is applied to tokamaks, the direction of the neoclassical impurity pinch is inward and thus the impurity

accumulation could be the major problem.

The major uncertainty of this scheme is the wall plasma interaction at high plasma temperature and its associated impurity contamination. Physical sputtering yield of D^+ ion to carbon tile has a peak value of ~ 2% at the incident energy of ~200 eV. Beyond this temperature, it gradually decreases down to 0.5% at 5 Kev. Considering that the total particle flux to the divertor plate is more than an order of magnitude lower than the conventional operation, physical sputtering due to D+ ion bombardment is not a problem. The issue may be unipolar arking, which used to be considered as a major impurity source in tokamak devices. It might occur at high divertor plasma temperature and definitely an experimental test for it is needed.

At temperature above 100 eV, secondary electrons emitted from the divertor plate become a source of the cold particles, which lower the divertor plasma temperature. This effect can be included in γ [7] and γ is 7.8 without secondary electron emission and is ~10 when the secondary emission rate is 0.7. But when it exceeds 0.7, γ increases rapidly and then saturates at ~23 because of the space charge limit. Selection of the divertor plate material in terms of secondary emission is important. When divertor plasma electrons become collisionless, i.e. the electron mean free path is much longer than the field line length between the divertor plates, secondary electrons emited from the divertor are first trapped barely by the sheath potential and makes oscillatory motion between the divertor plates. They eventually hit the divertor plate during the thermalization process. The parallel energy with which the secondary electrons hit the plates is ~0 and the perpendicular average energy is a fraction of the sheath potential in contrast to the previous collisional

model where both average striking energy are equal to T_e (the electron temperature). The sheath potential is ~ T_e when the secondary emission is limited by the space charge effect and thus the collisionless effect reduces the electron heat loss due to secondary electrons and hence γ significantly.

In the LHD experiment, we plan to install a cryopump system with overall pumping efficiency of ~20% in the divertor chamber. For a reactor, installation of the cryopump in the divertor region is unrealistic. We are trying to find divertor configurations which guide the heat and particle fluxes to a remote region, away from the main coil system, thereby making the particle pumping and the heat removal achievable even in a reactor system.

4. Conceptual design of the LHD helical divertor

The divertor design needs to be flexible so that one can accommodate a wide range of divertor operational scenarios. For this end, we design a largest possible vaccum vessel to accommodate closed divertor chambers within the budgetary and technical constraints.

One of the necessary conditions for divertor to function is that the scrape off layer plasma does not touch the wall surrounding the main plasma. The distance between the coil center and the plasma edge on the small major radius side of the torus is fairly small, 315mm. In order to increase clearance between the plasma and the wall, we decided to increase the coil current density up to 53A/mm^2, but it is still engineeringwise acceptable for reliable superconducting coil design. Because of the superconducting coil system, a radial space of 50 mm for the thermal insulation gap and the thermal displacement of the

components is needed, making the space there even tighter. After optimization of the system, the gap between the first wall and the plasma (the outermost edge surface layer) becomes 20mm for the standard configuration, a gap wide enough for effective divertor functions.

The majority of the heat and particle fluxes from the core are guided to the divertor plates installed in the divertor chamber as shown in Fig.1(h). Divertor performance depends on how well the neutral particles recycled at the divertor plates are controlled. The width of the entrance to the divertor chamber needs to be as small as possible for this reason. For the high density, cold divertor plasma operation, small entrance provides enhancement of recycling in the divertor, while keeping recycling at the main plasma edge minimal. For the high temperature divertor plasma operation, the pumping efficiency in the divertor chamber is the key parameter for the operation. The pumping efficiency is nearly equal to the ratio of the "equivalent" pump surface area to the entrance area. For the LHD experiment, we are considering pumping efficiency of ~20 %. A cryopump system will be used for the divertor pumping.

The divertor plates are the major divertor component which handles the heat flux from the core plasma. Its conceptual design has been completed. In the LHD divertor configuration, the direction of the magnetic field is nearly poloidal, thus eliminating a problem of high heat concentration at the tile edge caused by small misalignment of the tiles. All of four divertor legs have a three dimensional helical structure. From these facts, each divertor plate is designed as a helically running discrete-bar array instead of a continuous plane as in tokamaks. The angles between the field lines and the surfaces are designed to be around

30 degree at all the striking points. Each bar is made of copper cooling channel, on which several pieces of graphite or C-C composite armor are directly brazed. The cylindrical bar is 34~40 mm in diameter, 300~400 mm in length and a total of 2040 bars is necessary for covering all the striking points of the four divertor legs. Pressurized water cooling will be used to keep the surface temperature of the armor below 1200°C under the maximum heat flux of 10MW/m^2. High heat load tests of the C-Cu brazing for the LHD divertor plate have been initiated with an electron beam facility with 100KW. The results will be reported elsewhere.

Acknowledgement

We would like to express our particular appreciation to Drs. A. Iiyoshi, M. Fujiwara, J. Todoroki(NIFS), T. Obiki, J. Mizuuchi (Kyoto University) for their valuable comments and continuous encouragement.

References

(1) A. Iiyoshi, M. Fujiwara, O. Motojima, N. Ohyabu and K. Yamazaki, Fusion Technology 17 (1990) 169.

(2) F. Wagner, G. Becker, K. Behringer, D. Campbell, A. Eberhagen, et al., Phys. Rev. Lett. 49 (1982) 1408.

(3) M.Ali, Mahdavi, J.C. DeBoo, C.L. Hsieh, N. Ohyabu, R.D. Stambaugh, J.C. Wesley, Phys. Rev. Lett. 47 (1981) 1602.

(4) N. Ohyabu, Nucl. Fusion 21 (1981) 519.

(5) N. Ohyabu, Kakuyugo-Kenkyu 66 (1991) 525.

(6) K.S. Shaing, Phys. Fluids 26 (1983) 3164.

(7) G.D. Hobbs, J.A. Wesson, Plasma Phys. 9 (1967) 85.

Figure Captions

Fig. 1 Schematic view of the LHD helical divertor
(a) the poloidal crosssectional view with $\phi = 18^{\circ}$.
(b) the view along the helical coil.

Fig. 2 Edge magnetic configuration of a Heliotron/torsatron device which shows the magnetic structure clearly(it is not the LHD configuration). Puncture plot of the field lines at the poloidal plane with $\phi = 18^{\circ}$ and the field are traced forwards and backwards from the stochastic region just outside the closed surface.

Fig. 3 (a) Edge surface layer (at $\phi = 18^{\circ}$ poloidal plane) generated by tracing field lines forwards. Two X-points are located on the midplane at θ (the poloidal angle) = 0 and $\theta = \pi$ and are denoted by +.
(b) To illustrate the movement of the field lines in the edge surface layers clearly as they move toroidally, the locations of five field lines (A,B,C,D,E) are depicted at the poloidal planes with five different toroidal angles (from top to bottom, $\phi = 18^{\circ}, 54^{\circ}, 90^{\circ}, 126^{\circ}, 162^{\circ}$). However, it is not an exact field line tracing.

Fig. 4 A simplified power balance in the high temperature divertor plasma operation.

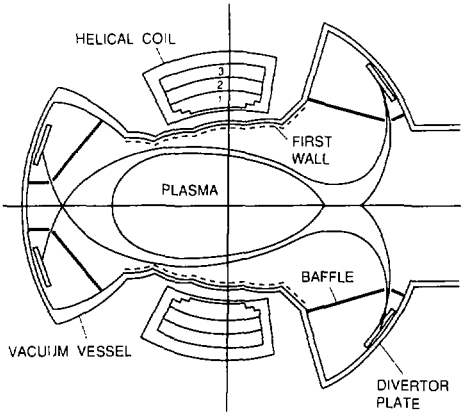
HELICAL COIL
3
2
1
FIRST WALL
PLASMA
BAFFLE
VACUUM VESSEL
DIVERTOR PLATE

(a)

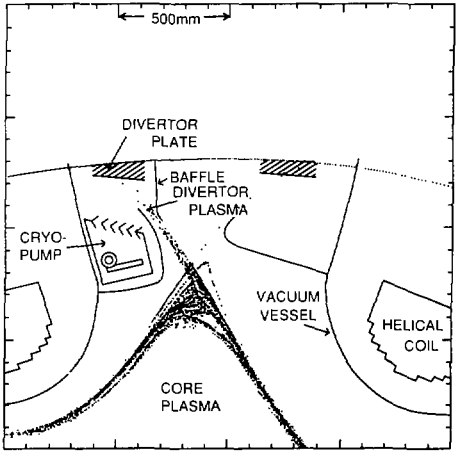
500mm
DIVERTOR PLATE
BAFFLE
DIVERTOR PLASMA
CRYO-PUMP
VACUUM VESSEL
HELICAL COIL
CORE PLASMA

(b)

Fig. 1

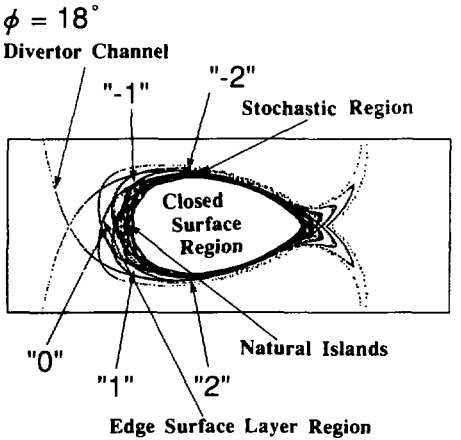
$\phi = 18^\circ$
Divertor Channel
"-1"
"-2"
Stochastic Region
Closed
Surface
Region
"0"
"1"
"2"
Natural Islands
Edge Surface Layer Region

Fig. 2

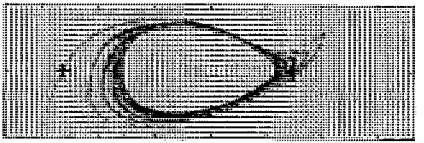

(a)

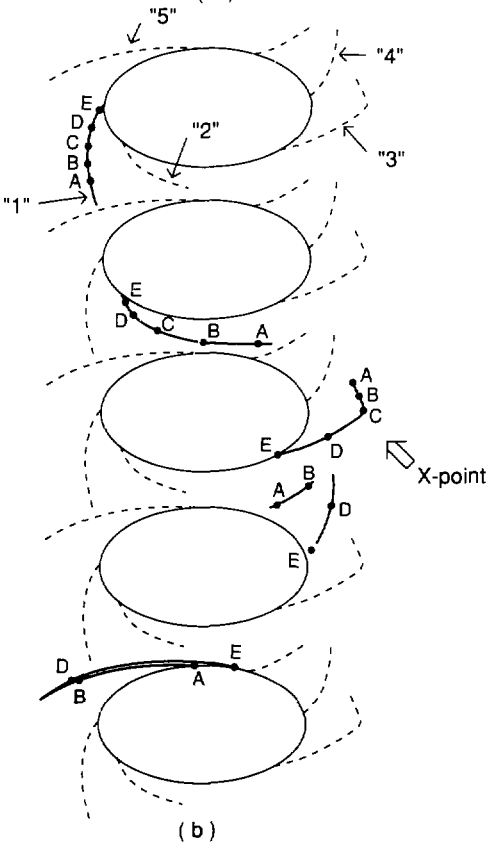

(b)

Fig. 3

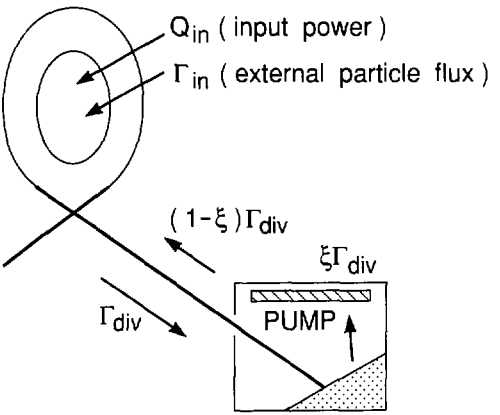
Q_{in} (input power)
Γ_{in} (external particle flux)
$(1-\xi)\Gamma_{div}$
$\xi\Gamma_{div}$
Γ_{div}
PUMP

Fig. 4

Recent Issues of NIFS Series

NIFS-93 Y. Miura, K. Itoh, S. - I. Itoh, T. Takizuka, H. Tamai, T. Matsuda, N. Suzuki, M. Mori, H. Maeda and O. Kardaun, *Geometric Dependence of the Scaling Law on the Energy Confinement Time in H-mode Discharges;* Jun. 1991

NIFS-94 H. Sanuki, K. Itoh, K. Ida and S. - I. Itoh, *On Radial Electric Field Structure in CHS Torsatron / Heliotron;* Jun. 1991

NIFS-95 K. Itoh, H. Sanuki and S. - I. Itoh, *Influence of Fast Ion Loss on Radial Electric Field in Wendelstein VII-A Stellarator;* Jun. 1991

NIFS-96 S. - I. Itoh, K. Itoh, A. Fukuyama, *ELMy-H mode as Limit Cycle and Chaotic Oscillations in Tokamak Plasmas;* Jun. 1991

NIFS-97 K. Itoh, S. - I. Itoh, H. Sanuki, A. Fukuyama, *An H-mode-Like Bifurcation in Core Plasma of Stellarators;* Jun. 1991

NIFS-98 H. Hojo, T. Watanabe, M. Inutake, M. Ichimura and S. Miyoshi, *Axial Pressure Profile Effects on Flute Interchange Stability in the Tandem Mirror GAMMA 10;* Jun. 1991

NIFS-99 A. Usadi, A. Kageyama, K. Watanabe and T. Sato, *A Global Simulation of the Magnetosphere with a Long Tail : Southward and Northward IMF;* Jun. 1991

NIFS-100 H. Hojo, T. Ogawa and M. Kono, *Fluid Description of Ponderomotive Force Compatible with the Kinetic One in a Warm Plasma* ; July 1991

NIFS-101 H. Momota, A. Ishida, Y. Kohzaki, G. H. Miley, S. Ohi, M. Ohnishi K. Yoshikawa, K. Sato, L. C. Steinhauer, Y. Tomita and M. Tuszewski *Conceptual Design of D-^{3}He FRC Reactor "ARTEMIS"* ; July 1991

NIFS-102 N. Nakajima and M. Okamoto, *Rotations of Bulk Ions and Impurities in Non-Axisymmetric Toroidal Systems* ; July 1991

NIFS-103 A. J. Lichtenberg, K. Itoh, S. - I. Itoh and A. Fukuyama, *The Role of Stochasticity in Sawtooth Oscillation* ; Aug. 1991

NIFS-104 K. Yamazaki and T. Amano, *Plasma Transport Simulation Modeling for Helical Confinement Systems;* Aug. 1991

NIFS-105 T. Sato, T. Hayashi, K. Watanabe, R. Horiuchi, M. Tanaka, N. Sawairi and K. Kusano, *Role of Compressibility on Driven Magnetic*

Reconnection ; Aug. 1991

NIFS-106 Qian Wen - Jia, Duan Yun - Bo, Wang Rong - Long and H. Narumi, *Electron Impact Excitation of Positive Ions - Partial Wave Approach in Coulomb - Eikonal Approximation* ; Sep. 1991

NIFS-107 S. Murakami and T. Sato, *Macroscale Particle Simulation of Externally Driven Magnetic Reconnection;* Sep. 1991

NIFS-108 Y. Ogawa, T. Amano, N. Nakajima, Y. Ohyabu, K. Yamazaki, S. P. Hirshman, W. I. van Rij and K. C. Shaing, *Neoclassical Transport Analysis in the Banana Regime on Large Helical Device (LHD) with the DKES Code;* Sep. 1991

NIFS-109 Y. Kondoh, *Thought Analysis on Relaxation and General Principle to Find Relaxed State;* Sep. 1991

NIFS-110 H. Yamada, K. Ida, H. Iguchi, K. Hanatani, S. Morita, O. Kaneko, H. C. Howe, S. P. Hirshman, D. K. Lee, H. Arimoto, M. Hosokawa, H. Idei, S. Kubo, K. Matsuoka, K. Nishimura, S. Okamura, Y. Takeiri, Y. Takita and C. Takahashi, *Shafranov Shift in Low-Aspect-Ratio Heliotron / Torsatron CHS* ; Sep 1991

NIFS-111 R. Horiuchi, M. Uchida and T. Sato, *Simulation Study of Stepwise Relaxation in a Spheromak Plasma* ; Oct. 1991

NIFS-112 M. Sasao, Y. Okabe, A. Fujisawa, H. Iguchi, J. Fujita, H. Yamaoka and M. Wada, *Development of Negative Heavy Ion Sources for Plasma Potential Measurement* ; Oct. 1991

NIFS-113 S. Kawata and H. Nakashima, *Tritium Content of a DT Pellet in Inertial Confinement Fusion* ; Oct. 1991

NIFS-114 M. Okamoto, N. Nakajima and H. Sugama, *Plasma Parameter Estimations for the Large Helical Device Based on the Gyro-Reduced Bohm Scaling* ; Oct. 1991

NIFS-115 Y. Okabe, *Study of Au^- Production in a Plasma-Sputter Type Negative Ion Source* ; Oct. 1991

NIFS-116 M. Sakamoto, K. N. Sato, Y. Ogawa, K. Kawahata, S. Hirokura, S. Okajima, K. Adati, Y. Hamada, S. Hidekuma, K. Ida, Y. Kawasumi, M. Kojima, K. Masai, S. Morita, H. Takahashi, Y. Taniguchi, K. Toi and T. Tsuzuki, *Fast Cooling Phenomena with Ice Pellet Injection in the JIPP T-IIU Tokamak*, Oct. 1991

NIFS-117 K. Itoh, H. Sanuki and S. I. Itoh, *Fast Ion Loss and Radial Electric Field in Wendelstein VII*

A Stellarator; Oct. 1991

NIFS-118 Y. Kondoh and Y. Hosaka, *Kernel Optimum Nearly-analytical Discretization (KOND) Method Applied to Parabolic Equations <<KOND-P Scheme>>*, Nov. 1991

NIFS-119 T. Yabe and T. Ishikawa, *Two- and Three-Dimensional Simulation Code for Radiation-Hydrodynamics in ICF*; Nov. 1991

NIFS-120 S. Kawata, M. Shiromoto and T. Teramoto, *Density-Carrying Particle Method for Fluid* ; Nov. 1991

NIFS-121 T. Ishikawa, P. Y. Wang, K. Wakui and T. Yabe, *A Method for the High-speed Generation of Random Numbers with Arbitrary Distributions;* Nov. 1991

NIFS-122 K. Yamazaki, H. Kaneko, Y. Taniguchi, O. Motojima and LHD Design *Group, Status of LHD Control System Design : Dec. 1991*

NIFS-123 Y. Kondoh, *Relaxed State of Energy in Incompressible Fluid and Incompressible MHD Fluid* ; Dec. 1991

NIFS-124 K. Ida, S. Hidekuma, M. Kojima, Y. Miura, S. Tsuji, K. Hoshino, M. Mori, N. Suzuki, T. Yamauchi and JFT-2M Group, *Edge Poloidal Rotation Profiles of H-Mode Plasmas in the JFT-2M Tokamak* ; Dec. 1991

NIFS-125 H. Sugama and M. Wakatani, *Statistical Analysis of Anomalous Transport in Resistive Interchange Turbulence* ;Dec. 1991

NIFS-126 K. Narihara, *A Steady State Tokamak Operation by Use of Magnetic Monopoles* ; Dec. 1991

NIFS-127 K. Itoh, S.-I. Itoh and A. Fukuyama, *Energy Transport in the Steady State Plasma Sustained by DC Helicity Current Drive* ;Jan. 1992

NIFS-128 Y. Hamada, Y. Kawasumi, K. Masai, H. Iguchi, A. Fujisawa, JIPP T-IIU Group and Y. Abe, *New High Voltage Parallel Plate Analyzer* ; Jan. 1992

NIFS-129 K. Ida and T. Kato, *Line-Emission Cross Sections for the Charge-exchange Reaction between Fully Stripped Carbon and Atomic Hydrogen in Tokamak Plasma*; Jan. 1992

NIFS-130 T. Hayashi, A. Takei and T. Sato, *Magnetic Surface Breaking in 3D MHD Equilibria of l=2 Heliotron* ; Jan. 1992

NIFS-131 K. Itoh, K. Ichiguchi and S.-I. Itoh, *Beta Limit of Resistive Plasma in Torsatron Heliotron* : Feb. 1992

NIFS-132 K. Sato and F. Miyawaki, *Formation of Presheath and Current-Free Double Layer in a Two-Electron-Temperature Plasma* : Feb. 1992

NIFS-133 T. Maruyama and S. Kawata, *Superposed-Laser Electron Acceleration* Feb. 1992

NIFS-134 Y. Miura, F. Okano, N. Suzuki, M. Mori, K. Hoshino, H. Maeda, T. Takizuka, JFT-2M Group, S.-I. Itoh and K. Itoh, *Rapid Change of Hydrogen Neutral Energy Distribution at L H-Transition in JFT-2M H-mode* ; Feb. 1992

NIFS-135 H. Ji, H. Toyama, A. Fujisawa, S. Shinohara and K. Miyamoto *Fluctuation and Edge Current Sustainment in a Reversed-Field-Pinch;* Feb. 1992

NIFS-136 K. Sato and F. Miyawaki, *Heat Flow of a Two-Electron-Temperature Plasma through the Sheath in the Presence of Electron Emission;* Mar. 1992

NIFS-137 T. Hayashi, U. Schwenn and E. Strumberger, *Field Line Diversion Properties of Finite β Helias Equilibria;* Mar. 1992

NIFS-138 T. Yamagishi, *Kinetic Approach to Long Wave Length Modes in Rotating Plasmas;* Mar. 1992

NIFS-139 K. Watanabe, N. Nakajima, M. Okamoto, Y. Nakamura and M. Wakatani, *Three-dimensional MHD Equilibrium in the Presence of Bootstrap Current for Large Helical Device (LHD);* Mar. 1992

NIFS-140 K. Itoh, S.-I. Itoh and A. Fukuyama, *Theory of Anomalous Transport in Toroidal Helical Plasmas;* Mar. 1992

NIFS-141 Y. Kondoh, *Internal Structures of Self-Organized Relaxed States and Self-Similar Decay Phase;* Mar. 1992

NIFS-142 U. Furukane, K. Sato, K. Takiyama and T. Oda, *Recombining Processes in a Cooling Plasma by Mixing of Initially Heated Gas;* Mar. 1992

NIFS-143 Y. Hamada, K. Masai, Y. Kawasumi, H. Iguchi, A. Fijisawa and JIPP T-IIU Group, *New Method of Error Elimination in Potential Profile Measurement of Tokamak Plasmas by High Voltage Heavy Ion Beam Probes;* Apr. 1992